Proceedings of the 2016 Joint Rail Conference
JRC2016
April 12-15, 2016, Columbia, SC, USA

JRC2016-5783

ESTIMATING DETERIORATION IN THE CONCRETE TIE-BALLAST INTERFACE BASED ON VERTICAL TIE DEFLECTION PROFILE: A NUMERICAL STUDY

Hailing Yu
Structures and Dynamics Division
John A. Volpe National Transportation Systems Center
U.S. Department of Transportation
Cambridge, MA 02142, U.S.A.

ABSTRACT

In ballasted concrete tie track, the tie-ballast interface can deteriorate resulting in concrete tie bottom abrasion, ballast pulverization and/or voids in tie-ballast interfaces. Tie-ballast voids toward tie ends can lead to unfavorable center binding support conditions that can result in premature concrete tie failure and possible train derailment. Direct detection of these conditions is difficult. There is a strong interest in assessing the concrete tie-ballast interface conditions indirectly using measured vertical deflections.

This paper seeks to establish a link between the vertical deflection profile of a concrete tie top surface and the tie-ballast interface condition using the finite element analysis (FEA) method. The concrete tie is modeled as a concrete matrix embedded with prestressing steel strands or wires. The configurations of two commonly used concrete ties, one with 8 prestressing strands and the other with 20 prestressing wires, are employed in this study. All models are three-dimensional and symmetric about the tie center. A damaged plasticity model that can predict onset and propagation of tensile cracks is applied to the concrete material. The steel-concrete interface is homogenized and represented with a thin layer of cohesive elements sandwiched between steel and concrete elements. Strand- or wire-specific elasto-plastic bond models developed at the Volpe Center are applied to the cohesive elements to account for the interface bonding mechanisms. FE models are developed for both original and worn concrete ties, with the latter assuming hypothetical patterns of reduced cross sections resulting from abrasive interactions with the ballast. Static analyses of pretension release in these concrete ties are conducted, and vertical deflection gradients along tie lengths are calculated and shown to correspond well with the worn cross sectional patterns for a given reinforcement type.

The ballast is further modeled with Extended Drucker-Prager plasticity, and hypothetical voids are applied toward the tie ends along the concrete tie-ballast interface to simulate center binding support conditions. The distance range over which the concrete tie is supported in the center is variable and yields different center binding severity. Static simulations are completed with vertical rail seat loads applied on the concrete tie-ballast assembly. The influences of various factors on the vertical deflection profile, including tie type, vertical load magnitude, center binding severity, cross sectional material loss and prestress loss, are examined based on the FEA results.

The work presented in this paper demonstrates the potential of using the vertical deflection profile of concrete tie top surfaces to assess deteriorations in the tie-ballast interface. The simulation results further help to clarify minimum technical requirements on inspection technologies that measure concrete tie vertical deflection profiles.

INTRODUCTION

Railroads use concrete ties for improved durability performance and longer service lives, especially in heavy haul and high speed rail lines. However, a number of performance issues and failure modes [1] have negatively affected the in-service performance of concrete ties. Two of these failure modes, center negative flexural cracking and abrasion along the interface with ballast, are attributed to deteriorated concrete tie-ballast interface conditions. It is generally believed that these conditions result in concrete tie bottom abrasion, ballast pulverization, and center binding support conditions for concrete ties [2-3].

On July 18, 2013, a CSX freight train carrying municipal waste derailed on Metro-North's Hudson Division in Bronx, New York. Field investigations at the derailment site uncovered

This material is declared a work of the U.S. Government and is not subject to copyright protection in the United States.
Approved for public release. Distribution is unlimited.

significant concrete tie deterioration in the concrete tie-ballast interface [4-5]. Key observations were: pulverized but dry ballast was observed on the surface of the track, and removing concrete ties from the track further revealed trapped water in the fouled ballast; multiple concrete ties retrieved near the point of derailment showed different degrees of abrasion (material loss) at the ends and along the bottom; these concrete ties also displayed center negative cracking patterns typical of those developed under center binding ballast support conditions in which the center of a tie is supported while the ends behave like cantilever beams. The observed deterioration appeared to have built up over time, thus a window existed for detection and correction. Early detection of these issues may have prevented the derailment. An inspection technology that can detect and quantify this type of deterioration is highly desirable.

Existing technologies have been unable to directly assess the defects in the concrete tie-ballast interfaces. Optical methods cannot reach the obscure locations of the tie-ballast interfaces, and radar and sonic/ultrasonic methods may give qualitative indications but not quantitative data on defects, as the relative similarity in concrete and ballast properties makes it a challenge to distinguish their boundaries. As a result, there has been a growing interest in assessing the concrete tie-ballast interface conditions indirectly using concrete tie surface data measureable by traditional methods. The Federal Railroad Administration recently solicited proposals to develop inspection technologies that can measure vertical deflections of concrete tie top surfaces, which will then be used to assess deteriorations in the concrete tie-ballast interface [6].

It is well known that railroad ties can assume different deflection shapes under different ballast support conditions. Figure 1 shows two deflected tie shapes assumed by Kerr [7]. Although not explicitly expressed in the book, the two diagrams are believed to show deflected tie shapes under good (upper diagram) and center binding support conditions. The deflected tie shapes may be calculated from the classic beam theory by assuming a ballast pressure distribution under the tie for a specific support condition [7-8].

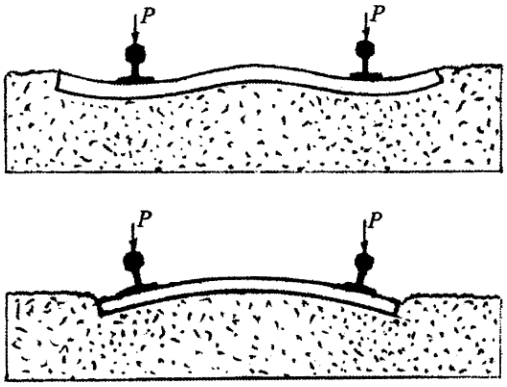

Figure 1: Assumptions of deflected tie shapes owing to different ballast support conditions (from [7]).

Recent advances in simulation technology using the finite element analysis (FEA) method enables more precise correlation of the concrete tie deflection profile with the concrete tie-ballast interface condition. The Volpe Center has developed realistic FE simulation models for pretensioned concrete crossties [9-10] and particularly interface bond models for various prestressing reinforcement types, including smooth wires, seven-wire strands and indented wires [11-13]. The FE model parameters were calibrated from extensive experimental data, and the model predictions of pretensioned concrete tie behavior were verified with test data.

Using these validated FE models, this research seeks to establish a link between the vertical deflection profile of a concrete tie and the tie-ballast interface condition. First, the FE modeling approach is described, including modeling of concrete tie, ballast and subgrade, validation cases, definition of center binding severity, description of vertical deflection and gradient, and simplifications adopted in the presented modeling approach. Vertical deflection profiles obtained using different variables are presented based on FE simulation results. Variables in unloaded and loaded conditions include tie type, vertical load magnitude, center binding severity, reduced cross sectional pattern and loss of prestress in the reinforcement. Conclusions are drawn based on the results presented in this paper, and implication of the FE results on inspection technology requirements for the concrete tie-ballast interface is discussed.

DESCRIPTION OF MODELING APPROACH

Volpe employed the commercial FE analysis software Abaqus/Standard in this study [14]. All models are three-dimensional and symmetric about the two center planes of the tie, resulting in quarter symmetric models. Pretension release and vertical loading processes were simulated statically.

Concrete Tie

Two concrete ties were considered in this study. As shown in Figure 2, Tie A has 8 prestressing strands, each made with seven wires, and Tie B has 20 prestressing wires. Their main geometric dimensions are summarized in Table 1. The seven-wire strands used in Tie A have a nominal diameter of 3/8 in. (9.525 mm), and the single wires in Tie B have a nominal diameter of 0.209 in. (5.32 mm). FE simulations have shown that including the scallops in Tie B only slightly changed the top surface deflections in loaded conditions, and therefore the scallops were not included in the simulations presented in this paper. Note that Tie A was modeled after the concrete ties recovered in the Metro North derailment [4-5].

The concrete ties were modeled as concrete matrixes embedded with prestressing steel strands or wires. A damaged plasticity model capable of predicting the onset and propagation of tensile cracks was applied to the concrete material [9-10]. The steel-concrete interface was homogenized and represented with a thin layer of cohesive elements sandwiched between steel and concrete elements. The cohesive elements followed elasto-plastic bond models developed for strand or wire reinforcements

[11-13]. The adhesive, frictional and dilatational bond model developed for seven-wire strands [12] was applied in the model of Tie A, whereas the bond model for the indented wire "WH" [13] was applied in the model of Tie B. The concrete and steel material parameters used in model development are summarized in Table 2, and the interface bond model parameters are summarized in Table 3. It is noted that the concrete properties of Tie B correspond to newly made concrete ties just reaching a compressive strength of nearly 6,000 psi (41.4 MPa), whereas the concrete material strengths of Tie A evolved over a long period of time and reached much higher values than those of Tie B. The more compliant concrete material would yield more significant top surface deflections. While the more compliant concrete material properties were employed for Tie B in this paper, more evolved material properties are expected for concrete ties that have been placed in track for some time.

The strands in Tie A were initially pretensioned to 17.25 kips (76.7 kN) per strand, equivalent to a nominal initial tensile stress of 156 ksi (1,075.6 MPa). The wires in Tie B were pretensioned to 7 kips (31.1 kN) per wire, equivalent to a nominal initial tensile stress of 203 ksi (1,399.6 MPa).

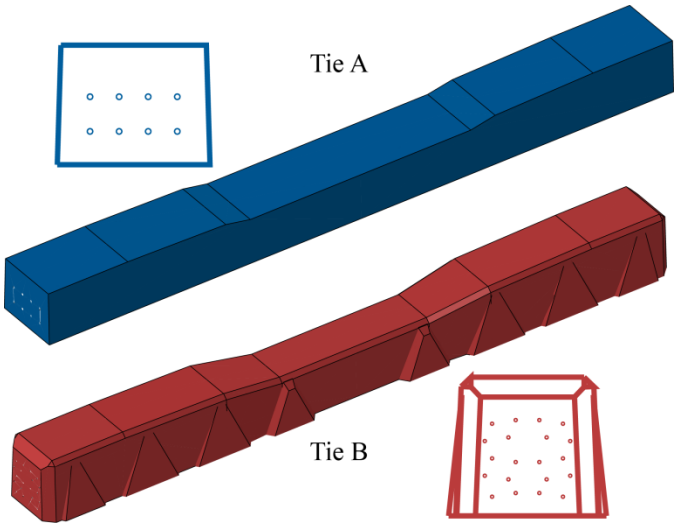

Figure 2: Concrete ties employed in this study.

Table 1. Concrete tie dimensions.

	Tie A	Tie B
Length	102 in. (2,590.8 mm)	
Length of center section	36 in. (914.4 mm)	24 in. (609.6 mm)
Height of center section	7 in. (177.8 mm)	7.5 in. (190.5 mm)
Height at rail seat center	8 in. (203.2 mm)	9.29 in. (236.0 mm)
Base width	10.5 in. (266.7 mm)	11 in. (279.4 mm)

Table 2. Concrete and steel material parameters.

Parameters	Tie A	Tie B	Steel
	Concrete Material		
Elastic modulus	4,941.0 ksi (34.1 GPa)	4,028 ksi (27.8 GPa)	30,000 ksi (206.8 GPa)
Poisson's ratio	0.202	0.2	0.3
Split tensile strength	1,012.5 psi (6.98 MPa)	478.8 psi (3.3 MPa)	-
Compressive strength	10,138.5 psi (69.9 MPa)	5977.8 psi (41.2 MPa)	-

Table 3. Interface bond model parameters.

Parameters	Seven-wire strand interface (Tie A)	Indented wire interface (Tie B)
D^{e}_{nn}	92,630,000 lbf/in^3 (25,144.1 N/mm^3)	12,889,494 lbf/in^3 (3,498.8 N/mm^3)
$D^{e}_{ns}(=D^{e}_{nt})$	385,958 lbf/in^3 (104.8 N/mm^3)	268,531 lbf/in^3 (72.9 N/mm^3)
$\tan\phi$	0.3	-
$\tan\psi$	0.0036	-
a_0	600 psi (4.14 MPa)	1000 psi (6.89 MPa)
u^{pl}_{tc}	0.08 in. (2.03 mm)	0.04 in. (1.02 mm)
u^{pl}_{td}	-	0.26 in. (6.60 mm)
u^{pl}_{ts}	-	0.27 in. (6.86 mm)
H_0	-	0.001 psi^{-1} (0.145 MPa^{-1})
H_1	-	0.018psi^{-1} (2.611 MPa^{-1})
μ^{max}_{d}	-	0.013

As discussed, the concrete ties recovered from the Metro North derailment showed significant material losses at the bottom of the ties [4-5]. Such material losses were accounted for in FEA through geometric modeling. Figure 3 shows field pictures and FE models of the end section of an unused and a worn concrete Tie A. The worn tie model had 1 in. (25.4 mm) of concrete material removed from the bottom across the length, approximately matching the most severe worn condition observed on the concrete ties in the field.

Figure 3: Field pictures and FE models of unused (left) and worn concrete Tie A (right) studied in the Metro North derailment investigation.

Ballast and Subgrade

The ballast was modeled with Extended Drucker-Prager plasticity suitable for simulating granular, frictional materials. The subgrade was modeled as an elastic half space. Figure 4 shows quarter symmetric ballast and subgrade models, and Table 4 shows the ballast and subgrade material parameters. The ballast and subgrade were modeled for a width equal to one tie spacing (or half tie spacing for quarter symmetric models). The subgrade is bounded by a hemi-cylindrical layer of infinite elements intended to simulate the infinite nature of the subgrade support. Infinite elements were assigned appropriately selected decay functions for their basic solution variables and designed to achieve far field solutions [15]. The tie spacing and ballast depth were assumed to be 30 in. (762 mm) and 24 in. (609.6 mm), respectively.

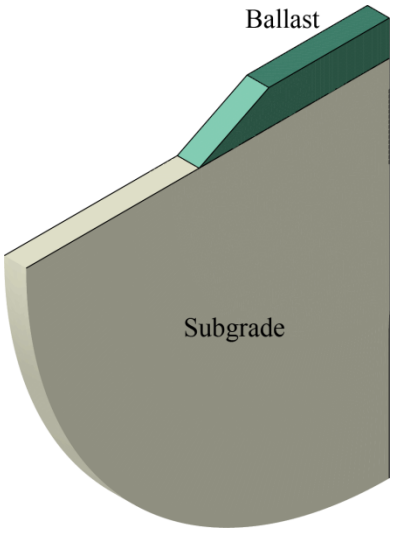

Figure 4: Quarter symmetric ballast and subgrade models.

Table 4. Ballast and subgrade material parameters.

Parameters	Ballast	Subgrade
Elastic modulus	30,168 psi (208 MPa)	72,519 psi (500 MPa)
Poisson's ratio	0.3	0.25
Yield strength	58 psi (400 KPa)	-

Notes on Model Validation

The Tie B model was validated with surface strain data measured on concrete ties made at a plant. The interface bond model used for Tie A was validated similarly. The Tie A model was further validated with data from the center negative moment test conducted on concrete ties retrieved at the July 18, 2013 Metro North derailment site.

The center negative moment test for monoblock concrete ties is specified in the American Railway Engineering and Maintenance-of-Way Association (AREMA) manual [16]. A diagram of the test is reproduced in Figure 5 for a 102 in. (2.59 m) tie. Five concrete ties retrieved at the Metro North derailment site and one unused concrete tie manufactured at the same time were tested according to this test specification, except that they were loaded to complete failure. The evolution of the load and the rail seat displacement (relative to the center cross section of the tie) was recorded. A detailed report on the tests and results can be found in Reference [17]. Figure 6 shows the force-relative rail seat displacement curves obtained from tests and FEA for the unused and a worn tie. The tests were not repeated so the test data shown were from a single test on each tie. The force quantity corresponds to the load P in Figure 5. The worn tie corresponds to Tie S3 in the Metro North derailment investigation [4-5,17]. The unused and worn tie models are the same as those shown in Figure 3. The force-relative rail seat displacement curves display an elastic phase followed by an elongated hardening phase with relatively large displacements. The concrete ties failed suddenly and catastrophically upon reaching the ultimate failure loads (maximum loads).

The FEA results represented by the solid green lines in Figure 6 used an initial pretension of 156 ksi (1,075.6 MPa) in the strands, and they consistently predicted higher force levels in the hardening phase than the test data for both unused and worn ties. Because both ties were about twenty years old, it was postulated that there were certain amounts of prestress loss in the strands. Although the exact amounts of prestress loss were unknown and difficult to quantify, Naaman [18] estimated that on average, the life time prestress loss due to time dependent effects such as shrinkage, creep and relaxation was 40 ksi (310.3 MPa) in stress relieved steel strands and 35 ksi (241.3 MPa) in low relaxation steel strands for normal weight concrete. Based on these data, an upper bound prestress loss amount of 40 ksi (310.3 MPa) was assumed, and the effect of the assumed prestress loss was achieved by reducing the initial pretension in the strands to 116 ksi (799.8 MPa) in a second set of simulations. The new FEA results incorporating prestress losses (dotted blue lines in Figure 6) showed more favorable comparisons with the test data.

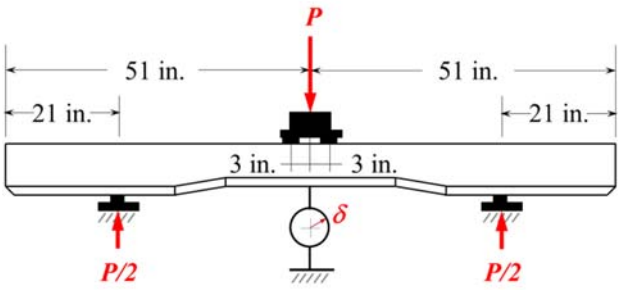

Figure 5: AREMA center negative moment test specification for monoblock concrete ties [16], reproduced for a 102 in. (2.59 m) tie (1 in. = 25.4 mm).

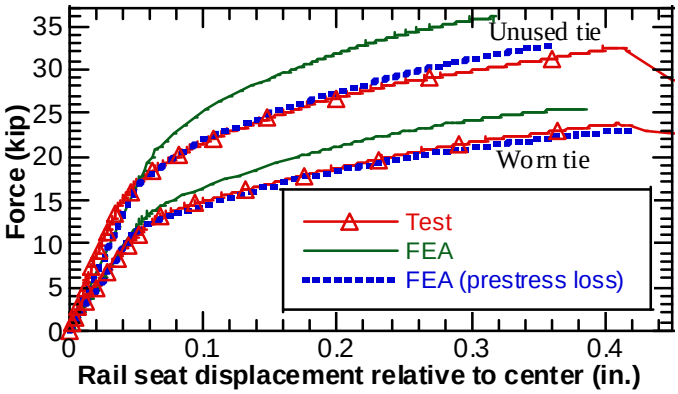

Figure 6: Force-relative rail seat displacement curves obtained from tests and FEA for unused and worn ties (1 kip = 4.448 kN, 1 in. = 25.4 mm).

Center Binding Severity

Center binding support conditions were simulated by applying voids toward the tie ends along the concrete tie-ballast interface. Figure 7 shows three hypothetical ballast support conditions depicted on a half symmetric lengthwise section of the tie and ballast. The two center binding conditions have full center support over just 20 and 48 in. (508 and 1,219.2 mm), respectively, in a full model out of the 102 in. (2.59 m) total tie length. Voids abutting the center support are applied and increase linearly in depth toward the tie ends. The largest vertical gap at the tie ends is 2 in. (50.8 mm) for the 20 in. (508 mm) center support and 1.317 in. (33.5 mm) for the 48 in. (1,219.2 mm) center support. The good support condition has full ballast support over the entire tie length. The distance range of the center support is thus variable and indicates different center binding severities, i.e., the narrower the center support, the more severe the center binding condition. The resultant force of the vertical pressure applied on each rail seat is denoted as $P/2$.

The ballast model was assigned homogeneous material properties as shown in Table 4. This was different from a ballast model previously used for similar studies where the ballast model was heterogeneous with three partitioned sections, each assigned different material parameters [19]. To assess the effect of the different ballast models, simulations were conducted on the two center binding conditions using both ballast models, and the force-relative displacement results are compared in Figure 8. The force quantity is equal to P, or two times the resultant rail seat force shown in Figure 7. The different ballast models did not appear to affect the maximum load level reached in the simulations or the overall response in the more severe center binding condition. In the less severe center binding scenario, there were larger relative rail seat displacements with the heterogeneous ballast, which may be partially attributed to the omitted ballast shoulder in the heterogeneous ballast modeling and consequently reduced confinement to movement.

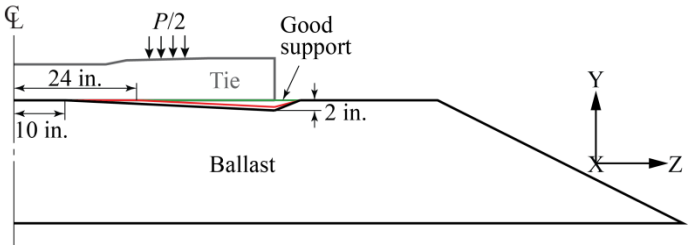

Figure 7: Hypothetical ballast support conditions in a half symmetric lengthwise section: two center binding scenarios (black and red outlines) due to deteriorated ballast and one good support condition (green outline) (1 in. = 25.4 mm).

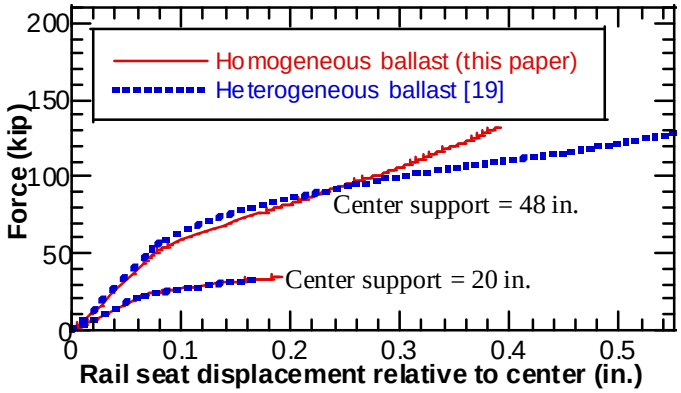

Figure 8: Force-relative rail seat displacement curves obtained from FEA using the homogeneous (this paper) or heterogeneous ballast model [19], with center support over 20 and 48 in. (508 and 1,219.2 mm), respectively (1 kip = 4.448 kN, 1 in. = 25.4 mm).

Vertical Deflection and Gradient

The primary interest of this study was with the vertical deflection profile of the top surface of the concrete tie. Using the global coordinate system shown in Figure 7, the top surface vertical deflection relative to the original undeformed shape along a lengthwise line (i.e., x=constant) is a function of the z-position along the tie length and may be expressed as

$$u_y = u_y(z) \tag{1}$$

The vertical deflection may be further calculated relative to the deflection on the center cross sectional plane z=0 and denoted as

$$u_{yc} = u_y(z) - u_y(z)\big|_{z=0} \quad (2)$$

Research into the vertical deflection data showed that the derivative of the vertical deflection along the tie length can highlight some important features of a deflection profile and therefore was useful in assessing the concrete tie-ballast interface condition. The term "gradient" was loosely used for the derivative of u_y along the z-direction and defined as

$$u_{y,z} = \frac{du_y(z)}{dz} = \frac{du_{yc}(z)}{dz} \approx \frac{\Delta u_y}{\Delta z} = \frac{\Delta u_{yc}}{\Delta z} \quad (3)$$

Simplifications

There were a few simplifications adopted in the modeling approach presented in this paper. The models were symmetric about the center cross section and therefore did not consider asymmetric conditions prevalent in the field. Secondly, only vertical rail seat loads were applied and thus the effect of lateral track loads was not studied. Further, the effect of ballast pulverization was indirectly simulated via applying voids in the tie-ballast interface, but the ballast material deterioration was not included in modeling. Despite these simplifications, the work in this paper was aimed at demonstrating the potential of using FEA to predict concrete tie vertical deflection and establishing a computational basis for linking the concrete tie vertical deflection with the tie-ballast interface condition.

VERTICAL DEFLECTION RESULTS

The vertical deflection profiles of Tie A and Tie B top surfaces were examined using FEA results based on the models defined in Figure 7. The studied factors include tie type, ballast support condition, vertical load magnitude, reduced concrete tie cross section and prestress loss in the reinforcement.

Effects of Tie Type, Ballast Support Condition and Vertical Load Magnitude

Figure 9(a) shows the concrete tie deflection profiles under the good ballast support condition defined in Figure 7. All the deflection profiles are shown for u_{yc} defined in Eq. (2), i.e., the vertical deflection relative to the center cross section of the tie. The P=0 cases correspond to the pretension released but unloaded tie conditions and indicate that the concrete ties are deflected even before any loads are applied.

Figure 9(a) also shows the loaded tie deflections. The results were examined at force levels of 20 and 30 kip (89.0 and 133.4 kN), respectively. When the Riks method [20] employed in the static analyses did not yield results at these prescribed force levels, linear interpolations were conducted to obtain results corresponding to these exact force magnitudes. For Tie B, the loaded deflection shapes shown in Figure 9(a) are similar to the unloaded one except for the indentations in the rail seat. For Tie A, the upward deflection in the unloaded condition changes to downward deflections when loaded, and the downward deflection increases with the applied load. The Tie A deflection resembles the tie shape predicted in the upper diagram of Figure 1 (good support condition), but the Tie B deflection deviates from it.

Figure 9(b) further plots the vertical deflections relative to the pretension released states by subtracting the deflection at P=0 from the deflections at P=20 or 30 kip for both Tie A and Tie B. This relative deflection quantity is denoted as $u_{yc\text{-}0}$. These relative deflections assume the shape predicted in the upper diagram of Figure 1 with the good support condition and indicate minimum differences between Tie A and Tie B. Note that the Tie B model was assigned the more compliant concrete material properties in Table 2; if the same evolved concrete material properties for Tie A were assigned instead, Tie B would show less vertical deflections under the same loading conditions.

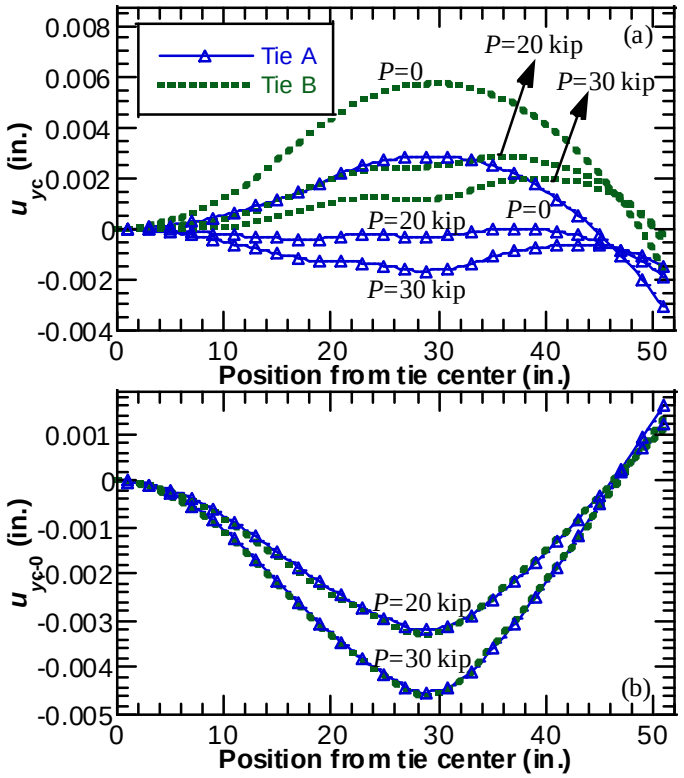

Figure 9: Good ballast support condition: (a) vertical deflection, and (b) vertical deflection relative to the pretension released state (subtracting the deflection at P=0) of concrete tie top surface along the tie length (1 kip = 4.448 kN, 1 in. = 25.4 mm).

Figure 10(a) shows the concrete tie deflection profiles under the two center binding ballast support conditions defined in Figure 7, again subjected to 20 and 30 kip vertical loads, respectively. Figure 10(a) indicates that both ties assume downward shapes relative to the center section, consistent with the prediction in Figure 1 (lower diagram). In addition, the tie deflection clearly increases with the applied load and the center binding severity. However, it is conceivable that a low load and high center binding severity combination can yield a similar

deflection profile as a high load and low center binding severity combination, in which case additional information on load magnitude may be needed to enable assessment of the ballast support condition. Further, the differences in the deflections of Tie A versus Tie B are not significant enough to help distinguish the type of tie being used.

Figure 10(b) plots the vertical deflection gradients calculated from Eq. (3) using the data shown in Figure 10(a). The gradients are mostly negative, and their magnitudes increase monotonically with the distance from the tie center. In particular, abrupt changes in gradients were observed for both Tie A and Tie B under the 30 kip (133.4 kN) load and 20 in. (508 mm) center support combination. To help understand the factors contributing to the abrupt gradient changes, the tensile damage variable contours were plotted and examined in Figure 11 for both ties.

The tensile damage variable d_t measures the degree of tensile strength degradation in concrete, with d_t=0 indicating undamaged concrete and d_t=1 indicating formation of cracks upon complete loss of the tensile strength. An examination of Figure 11 indicates that the abrupt gradient changes observed in Figure 10(b) correspond to locations with concentrated concrete damage and impending crack formations.

Effect of Reduced Concrete Tie Cross Section

As discussed, concrete ties can experience significant abrasion and consequent material losses at the interface with the ballast. To investigate the effect of these material losses, Tie A model was adapted to incorporate several hypothetical patterns of reduced cross sections, as shown in Figure 12, due to abrasion at the bottom. Each line near the tie bottom corresponds to a specific abrasion pattern, for which all of the concrete material below the line was removed from the model. Pattern A00 corresponds to the intact Tie A model. The first set of abrasion patterns, A01-A04, shows material losses near the tie end that also progressively propagate toward the tie center. The second set of abrasion patterns, A11-A55, shows material losses across the entire length of the tie, in addition to abrasion at the end. For A01-A04, the depth of material loss at the tie end ranged from 0.5-1.25 in. (12.7-31.75 mm) with 0.25 in. (6.35 mm) increments. For A11-A55, the depth of the material loss across the tie length ranged from 0.2-1.0 in. (5.08-25.4 mm) with 0.2 in. (5.08 mm) increments.

Concrete ties with bottom abrasions are often associated with center binding support conditions and when loaded, deflect in similar manners as shown in Figure 10. The reduced cross sections generally lead to larger downward deflections and higher negative gradients in loaded conditions. They also change the deflection profile in the pretension released but unloaded state. Figure 13 shows the vertical deflection gradients for Tie A with abrasion patterns defined in Figure 12 in a pretension released but unloaded state. There appears to be a distinguishing profile for each abrasion pattern, meaning the data can be used to assess the extent of concrete tie bottom abrasion.

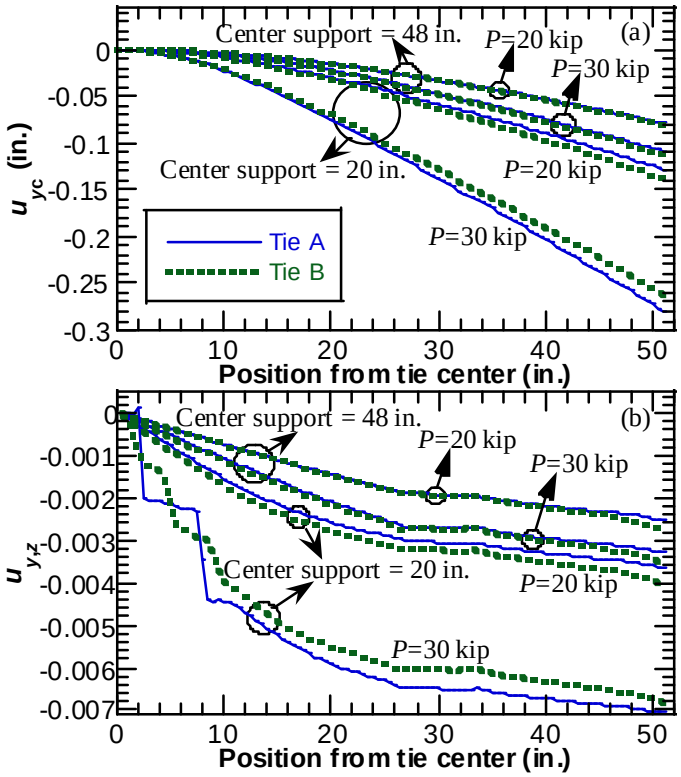

Figure 10: Center binding ballast support conditions: (a) vertical deflection, and (b) vertical deflection gradient (1 kip = 4.448 kN, 1 in. = 25.4 mm).

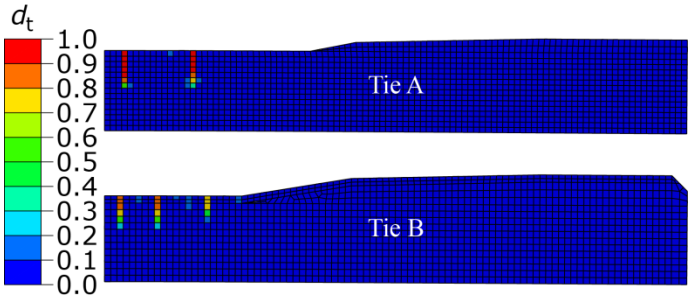

Figure 11: Tensile damage variable contours for Tie A and Tie B subjected to a vertical load *P*=30 kip (133.4 kN) under the 20 in. (508 mm) center support condition.

Figure 12: Hypothetical abrasion or material loss patterns at the bottom of Tie A.

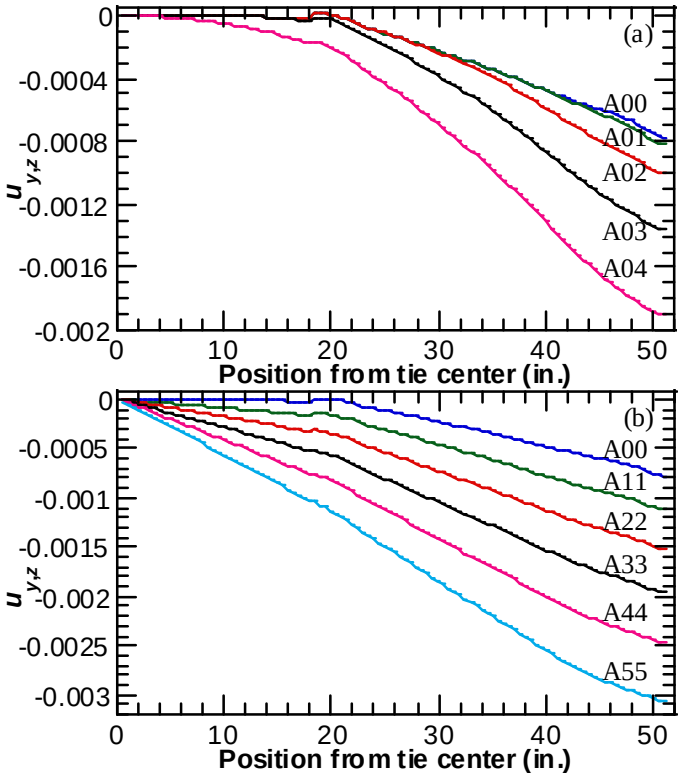

Figure 13: Vertical deflection gradient along the tie length in a pretension released but unloaded state for the abrasion patterns defined in Figure 12: (a) A00-A04, and (b) A00-A55 (1 in. = 25.4 mm).

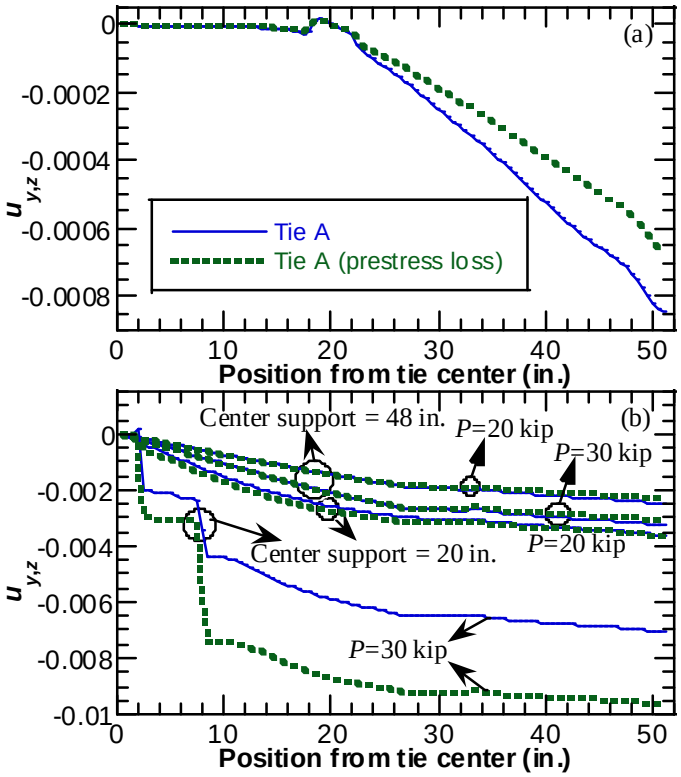

Figure 14: Vertical deflection gradient along the tie length for Tie A in normal condition or with prestress loss in (a) pretension released but unloaded state, and (b) loaded states (1 kip = 4.448 kN, 1 in. = 25.4 mm).

Effect of Prestress Loss in Reinforcement

The validation of Tie A model in the center negative flexural mode showed that the prestress loss in the steel reinforcements over time can affect the tie's flexural response. The effect of prestress loss on the vertical deflection profile was further studied. Figure 14 shows the vertical deflection gradients of Tie A's top surface with two prestress specifications in the steel strands: the regular 156 ksi (1,075.6 MPa) and the lower 116 ksi (799.8 MPa) representing a 40 ksi (310.3 MPa) loss. Deflection gradients in both unloaded and loaded center binding conditions are plotted.

Figure 14(a) shows insignificant differences in the vertical deflection gradient in the pretension released but unloaded state, without or with prestress loss in the strands. Figure 14(b) shows that the same was mostly true when the tie was loaded under the two center binding conditions. The only exception was that under 30 kip (133.4 kN) vertical load and 20 in. (508 mm) center support, the negative deflection gradient was much larger for the tie with prestress loss than for the one with regular prestress in the strands. In this state, both ties also displayed concentrated damage with impending crack formation.

CONCLUSIONS

Despite a few simplifications adopted in the study, the FEA results presented in this paper demonstrate that it is possible to use the vertical deflection profile of concrete tie top surfaces to assess tie-ballast interface conditions, including tie abrasion at the ballast interface and center binding support resulting from deteriorated ballast. The vertical deflection gradient is further shown to highlight critical features such as concentrated damage and crack formation in the concrete ties.

The FEA results indicate that the vertical deflection profile in the pretension released but unloaded state can be used to discern the extent of bottom abrasion. However, it is not sufficient for evaluating the loss of prestress in the steel reinforcements.

When loaded under a good ballast support condition, the deflected tie shape does not always match the classical prediction, but the deflection profiles are distinctively different for the two types of concrete ties studied. However, if the deflections in the pretension released but unloaded state were subtracted from the loaded deflections, the resulting profiles both match the classical prediction and show minimal differences between the two ties under study.

When loaded under two hypothetical center binding support conditions, the deflected tie shape generally matches the classical prediction, but the deflection profiles are insignificantly different for the two concrete ties under similar loading and

support conditions. Further, the downward deflection increases with both the vertical load magnitude and the center binding severity, meaning additional knowledge on the load magnitude will help to more accurately assess center binding severity resulting from deteriorated ballast.

Based on the results presented in this paper, inspection technologies capable of measuring concrete tie vertical deflections as small as 1 mil (one-thousandth of an inch) have the potential to capture detailed features of the deflection profiles. Further, the lengthwise resolution of the deflection data should be sufficiently small in order to obtain meaningful derivatives (or gradients) of the deflections.

ACKNOWLEDGEMENT

The work described in this paper was sponsored by the Office of Research, Development and Technology, Federal Railroad Administration, U.S. Department of Transportation. Directions provided by Messrs. Gary Carr and Cameron Stuart of the Track Research Division are gratefully acknowledged. The author benefited tremendously from technical discussions with Brian Marquis, David Jeong and Mike Coltman of the Volpe Center. Mike Carolan of the Volpe Center helped to improve the geometry of the ballast model.

REFERENCES

[1] Yu, H., Jeong, D., Marquis, B., and Coltman, M., 2015, "Railroad Concrete Tie Failure Modes and Research Needs," 2015 Transportation Research Board 94th Annual Meeting, TRB15-0311.

[2] Lutch, R. H., Harris, D. K., and Ahlborn, T. M. "Prestressed concrete ties in North America," AREMA Conference, 2009.

[3] Lutch, R. H., 2009, Capacity Optimization of a Prestressed Concrete Railroad Tie, Master Thesis, Michigan Technological University.

[4] National Transportation Safety Board, 2014, "Railroad Accident Brief – Metro-North Railroad Derailment," Report No. NTSB/RAB-14/11.

[5] Marquis, B., LeBlanc, J., Yu, H., and Jeong D., 2014, "CSX Derailment on Metro-North Tracks in Bronx, NY, July 18, 2013," Report to National Transportation Safety Board, http://dms.ntsb.gov/pubdms/search/document.cfm?docID=417234&docketID=55312&mkey=87518

[6] Federal Railroad Administration, 2015, Broad Agency Announcement, Appendix C - Research Topics.

[7] Kerr, A. D., 2003, Fundamentals of Railway Track Engineering, Simmons-Boardman Books, Inc.

[8] Hanna, A. N., 1979, "State-of-the-art report on prestressed concrete ties for North American railroads," PCI Journal, pp. 32-61.

[9] Yu, H., Jeong, D. Y., Choros, J., and Sussmann, T., 2011, "Finite Element Modeling of Prestressed Concrete Crossties with Ballast and Subgrade Support." Proc. ASME 2011 International Design Engineering Technical Conferences & Computers and Information in Engineering Conference, DETC2011-47452.

[10] Yu, H., and Jeong, D. Y., 2012, "Railroad Tie Responses to Directly Applied Rail Seat Loading in Ballasted Tracks: A Computational Study," Proc. ASME/ASCE/IEEE 2012 Joint Rail Conference, JRC2012-74149.

[11] Yu, H., and Jeong, D. Y., 2014, "Bond between Smooth Prestressing Wires and Concrete: Finite Element Model and Transfer Length Analysis for Pretensioned Concrete Crossties," Proceedings of the 2014 ASCE Structures Congress.

[12] Yu, H., and Jeong, D.Y., 2015, "Finite Element Bond Models for Seven-Wire Prestressing Strands in Concrete Crossties," Proceedings of the 2015 Joint Rail Conference, JRC2015-5758.

[13] Yu, H., and Jeong, D.Y., 2016, "Finite Element Bond Modeling for Indented Wires in Pretensioned Concrete Crossties," 2016 Joint Rail Conference, JRC2015-5782.

[14] Dassault Systèmes, Abaqus Analysis User's Manual, 2012.

[15] Dassault Systèmes, Abaqus Theory Manual, 2012.

[16] American Railway Engineering and Maintenance-of-Way Association, 2010, Manual for Railway Engineering, Chapter 30, Part 4: Concrete Ties.

[17] Wiss, Janney, Elstner Associates, 2014, "Concrete Tie Testing and Petrographic Services," Report No. NTSB-R-140003.

[18] Naaman, A. E., 2012, Prestressed Concrete Analysis and Design: Fundamentals, 3rd ed., Techno Press 3000.

[19] Yu, H., Marquis, B., and Jeong, D.Y., "Failure Analysis of Railroad Concrete Crossties in Center Binding Conditions Using Finite Element Method," Proceedings of the Stephenson Conference, Institution of Mechanical Engineers, London, UK, April 21-23, 2015.

[20] Riks, E., 1979, "An incremental approach to the solution of snapping and buckling problems," International Journal of Solids and Structures, 15(7), pp. 529-551.